

## Some dynamical characteristics and thermal structure of monsoon depressions over the Bay of Bengal

By S. RAJAMANI\* and D. N. SIKDAR, *Department of Geosciences, The University of Wisconsin-Milwaukee, Milwaukee, Wisconsin 53201, USA*

(Manuscript received 31 March 1987; in final form 29 July 1988)

### ABSTRACT

In this paper, some of the dynamical characteristics and the thermal structure of the monsoon depressions formed during July–August 1979 in the Bay of Bengal are presented. The vorticity budget terms are examined for the eastern and western halves of three depressions in a Lagrangian reference frame. Two of the depressions moved westward and one northward. The vorticity divergence term and the horizontal advection term (in the upper troposphere) apparently caused the westward movement, whereas the vertical advection term and tilting term had little influence on the movement. The residual term is predominantly negative in the western half of the monsoon depression where convective activity and rainfall are greater, compared to the eastern half. This corroborates the inference of Sui and Yanai that the appearance of large vorticity budget residuals is associated with intense cumulus convection. The computational study of energetics shows that the zonal available potential energy was the source for eddy available potential energy. This, in turn, was converted into eddy kinetic energy on most of the days during the life cycle of monsoon depressions. Eddy kinetic energy was converted into zonal kinetic energy on many days, thus maintaining the monsoon current. Computations of the momentum transport show that the transport was southward over the region 18°N to 25°N during the strengthening of the depressions and northward during the decaying stage. From analysis of thermal structure, the August depression (6–13 August 1979) had a warm core until two days after it reached peak intensity; subsequently it had a cold core.

### 1. Introduction

Since the MONEX 1979 data set became available, a number of studies were undertaken on various aspects of monsoon depressions. Examples are the studies by Sanders (1984), Saha and Shukla (1980), Surgi (1984), Nitta and Masuda (1981), Nitta and Murakami (1980), Sikka et al. (1980), Warner (1984). In this study, we examine the dynamical characteristics like vorticity budget, energetics and momentum transport, and also the thermal structure during the life cycle of monsoon depressions which formed during July–August 1979. To study the vorticity budget and the thermal structure, a

Lagrangian frame was adopted, in order to concentrate our attention on the area covering the monsoon depression/low, and moving with it from the time of its formation until its decay. The vorticity budget of monsoon depressions was studied by Krishnamurti et al. (1976), Daggupaty and Sikka (1977), Godbole (1977a, b), Surgi (1984) and Douglas (1987) and that in case of extratropical systems by DiMego and Bosart (1982), Chen and Chang (1980), Sui and Yanai (1986) and others.

Monsoon depressions cause most monsoon rains (Rao, 1976, p. 107) and their tracks are responsible for shifting the rainfall regions as well as affecting the general monsoon activity. For example, if their tracks lie between westward and northwestward, the rainfall would occur over most parts of central India, and the general

\* On leave from Indian Institute of Tropical Meteorology, Pune, 411 005, India.

monsoon activity would continue to be intense. In contrast, if the tracks are northward, then the rainfall region shifts to northern India and the foothills of the Himalayas. This may even lead to break monsoon conditions by causing the shift of the monsoon trough to the north. Further details are available in Rao (1976) who exhaustively reviewed different types of synoptic situations during the summer monsoon (Krishnamurti, 1985).

It is important to understand what causes the depressions to sometimes move westward and at other times move northwards. We investigate this by computing all the terms in the vorticity equation over the depression area as well as over the eastern and western halves of the three depressions formed during July and August 1979. In order to understand the source of energy for various monsoon systems, the energetics and momentum transport were computed for the same period. We also examined how the temperature of the core of depressions varied during different stages of their life cycle.

## 2. Background

We investigated three monsoon depressions from India. The first which was studied in detail, was the remnant of the typhoon "Hope". This reached the northeastern Bay of Bengal as a well marked low-pressure system on 5 August 1979. It moved west-northwestward, reaching an intensity of a cyclonic storm on 7 August, with a central pressure of 984 mb at the surface, weakened during next few days, and ultimately merged with the seasonal low on 13 August at the border of northwestern India and Pakistan. The second depression formed as a low pressure area on 10 August, and intensified into a deep depression by 15 August, but on the next day it was observed only as a trough. The system moved slowly northward. A third system (Depression 3) which was formed on 4–5 July 1979 moved west-northwestwards. It reached maximum intensity on 7 July and by 10 July it became a weak low. Fig. 1 is an illustration of the tracks of the three systems obtained from the Indian Daily Weather Report published by the India Meteorological Department. The WMO (1981) contains many figures of typical synoptic situations, and includes

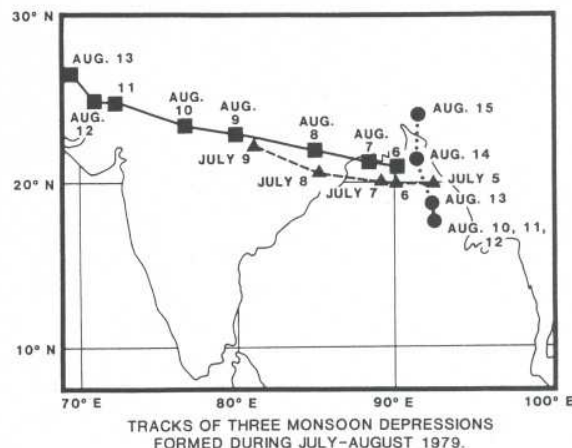


Fig. 1. Tracks of the three monsoon depressions formed during July–August 1979, and the area of study.

850 and 200 mb charts of 7 July and 7 August when the two depressions were most intense. For details of the daily weather summary from 1 June to 31 August 1979 see Sikka and Grossman (1980).

The winds and temperatures at the grid points from ECMWF analyses were utilized for this study. The grid size was  $1.875^\circ$ , and the area was from  $7.5^\circ\text{N}$  to  $30^\circ\text{N}$  and from  $69^\circ\text{E}$  to  $105^\circ\text{E}$ . Data at the standard levels, viz., 1000, 850, 700, 500, 400, 300, 250, 200, 150 and 100 mb levels for the periods from 4–16 August 1979 and from 1–10 July 1979 were used. The ECMWF analyses during the period from 1–10 July 1979 were based on conventional data, and the special observations taken by research aircraft from 1–10 July 1979, and research ships from the Soviet Union USSR in polygon formation from 8 July onwards. In other words, there was good data coverage for this period. However, the analyses for the period from 4–16 August 1979 were based on conventional data, and the data collected by two research ships from 6 August to 11–12 August over the Bay of Bengal. See WMO (1981) for detailed plots of vessel tracks.

For computations of vorticity budget and thermal structure, only the area of the depressions was considered. Since the depressions formed close to the land, observations in their vicinity were available for analyses. However, for the computations of monsoon energetics, the Bay of Bengal region was also included in these cases where the observations were relatively few.



### 3. Computations and discussion

#### 3.1. Relative vorticity and vertical velocity

The relative vorticity and the divergence were computed from wind fields 00 GMT and 12 GMT at all standard levels for the periods from 4–16 August 1979, and from 1–10 July 1979. The vertical velocity was also computed using the kinematic method. Relative vorticity and vertical velocity were averaged over the region ( $13^\circ$  longitude  $\times$   $11^\circ$  latitude) which covered the monsoon depression.

Vertical time sections for Depression 1 are depicted in Figs. 2a and 2b. The relative vorticity (mean value for the region of the depression) has a maximum value of  $3.3 \times 10^{-5} \text{ s}^{-1}$  at 700 mb level on 7 August when the system was most intense. The system contained a cyclonic vorticity of up to 200 mb on 7 August, and then tapered down to 700 mb for the seasonal low on 14, 15 August. Another important feature is that the system was most intense at 700 mb on all days until it merged with the seasonal low. The mean vertical velocity (Fig. 2b) associated with this system has a maximum value of  $170 \times 10^{-5} \text{ mb s}^{-1}$  or  $1.7 \text{ cm s}^{-1}$  on 7 August at 700 mb. Upward motion as large as  $500 \times 10^{-5} \text{ mb s}^{-1}$  or  $5 \text{ cm s}^{-1}$  was recorded at some gridpoints. The upward motion dominated the entire troposphere (with maximum values at 700 mb) until 12 August. After 12 August, there was downward motion in upper troposphere. In summary monsoon Depression 1 was most intense at 700 mb (Figs. 2a, b).

**3.1.1. Vorticity budget.** The vorticity budget for monsoon depression was studied by Daggupaty and Sikka (1977), Godbole (1977a), Surgi (1984) and others. Daggupaty and Sikka (1977) explained that the westward movement of the monsoon depression is due to the vorticity divergence term at the lower levels and due to cumulus scale features at the middle and upper levels. Godbole (1977a) found that cumulus-scale eddies work against the large-scale system and tend to offset the large scale imbalance in vorticity. Surgi (1984) suggested that the small difference between the forcings in the vorticity equation due to the horizontal advection and the cumulus scale eddies caused the westward movement of the depression.

In this study, the importance of the terms in

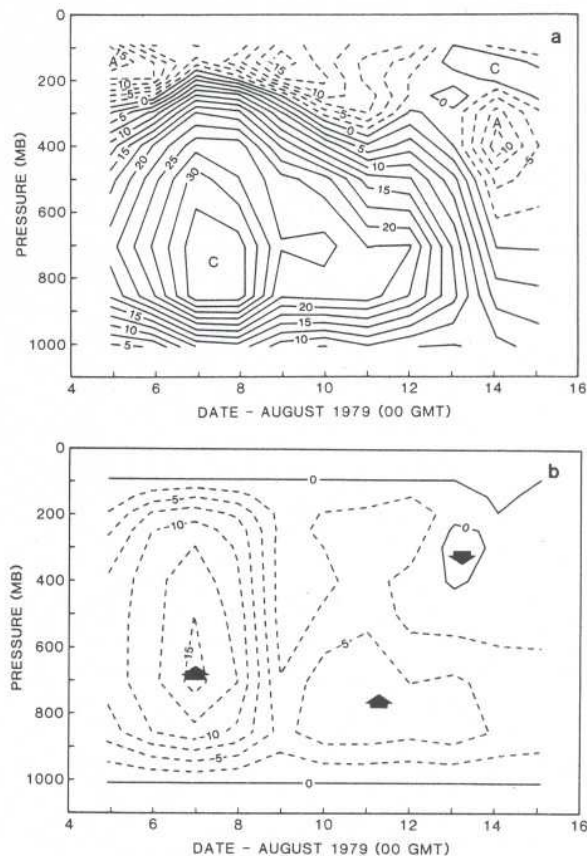


Fig. 2. Height-time section for Depression 1 (6–13 August 1979). (a) Relative vorticity ( $10^{-6} \text{ s}^{-1}$ ), and (b) vertical velocity ( $10^{-4} \text{ mb s}^{-1}$ ).

the vorticity equation (eq. 1) were considered, as was their influence on the movement of the depression.

The vorticity budget equation is:

$$\frac{\partial \zeta}{\partial t} + (\zeta + f) \nabla \cdot \mathbf{V} + \mathbf{V} \cdot \nabla (\zeta + f) + w \frac{\partial \zeta}{\partial p} + \left( \frac{\partial w}{\partial x} \frac{\partial v}{\partial p} - \frac{\partial w}{\partial y} \frac{\partial u}{\partial p} \right) = Z \quad (1)$$

I                      II  
III                      IV                      V

where  $Z$  is the residual term. All terms in eq. (1) were computed for the three depressions mentioned in Section 2. The terms were averaged over an area approximately  $13^\circ$  longitude  $\times$   $11^\circ$  latitude ( $7 \times 6$  grid lengths) covering the entire monsoon depression and moving with it from the time of its formation until its decay. Figs. 3a–c are plots of the vertical time section of vorticity

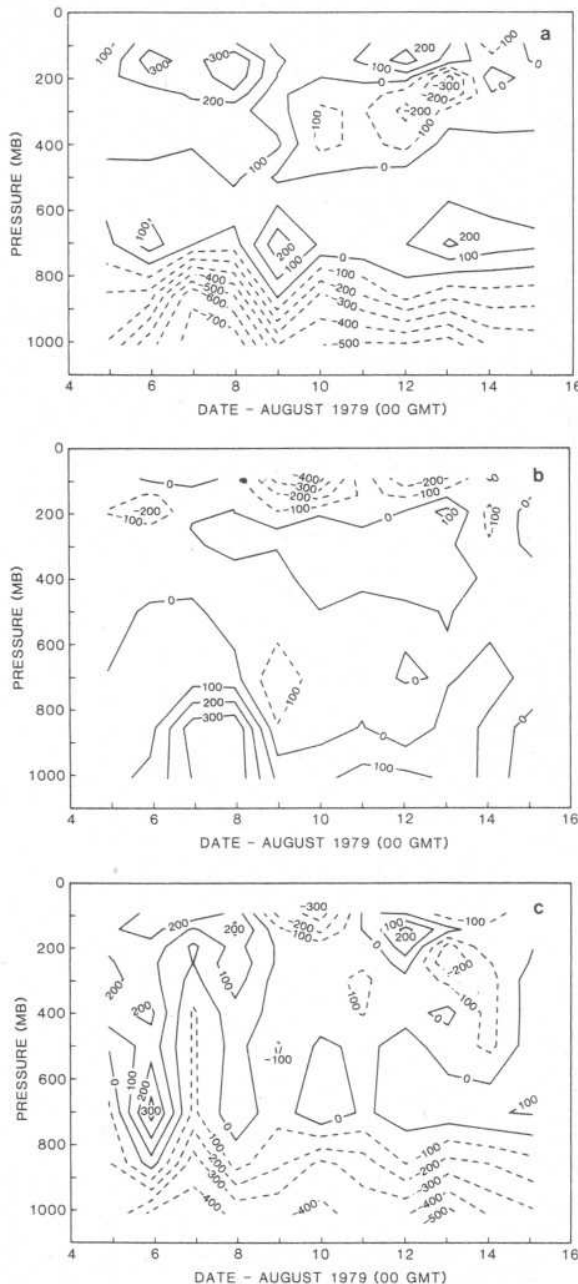


Fig. 3. Height-time section for Depression 1. Full area. (a) Vorticity divergence term, and (b) the horizontal advection term; (c) the residual term. The units are  $10^{-12} \text{ s}^{-2}$ .

divergence term (Term I in eq. (1)), horizontal advection term (Term II), and Z, the residual term (Term V), respectively for Depression 1 (6–13 August). For all terms, except for residual term, negative values would mean vorticity source and positive values would mean vorticity

sink. The vorticity divergence term is found to be a vorticity source at levels below 700 mb, as a vorticity sink above 700 mb except between the 400–200 mb level from 9 August onwards. The horizontal advection term, on the other hand, indicates a vorticity sink at low levels and a source at higher levels (Fig. 3b). The contributions by the vertical advection term in the vorticity budget equation and tilting term are comparatively small. However, when the depression is very active, their magnitudes become comparable with other terms in the vorticity budget equation and cannot be neglected. The vertical advection term causes a vorticity sink at levels below 700 mb and vorticity source above 700 mb, whereas the tilting term becomes vorticity source below 700 mb level and vorticity sink above. Douglas (1987) obtained similar features for 3–8 July 1979 (Depression 3) for the 500–300 layer that is, the vertical advection term act as a vorticity source, and the tilting term as a vorticity sink.

In most vorticity budget analyses made for the western Pacific, there is large positive residual (an apparent source of positive vorticity) in the upper troposphere and a negative residual (an apparent sink) in the lower troposphere (Sui and Yanai, 1986). Reed and Johnson (1974) for a composite easterly wave, Godbole (1977a) for a monsoon depression and Chen and Bosart (1979) for a composite cyclone obtained a residual term that was negative in the lower troposphere and positive in the upper troposphere. However, DiMego and Bosart (1982) observed during the reintensification stage of hurricane "Agnes" the residual term was negative (vorticity sink at all levels except the mid-level). In our study, the vertical time section of the residual term (Fig. 3c) is dominated by negative values suggestive of vorticity sink on most days. We attribute this to cumulus activity in the depression region. Sui and Yanai (1986) presented observational evidence for the association of the large vorticity residual term with cumulus convection in GATE region. They found in the horizontal distribution of the residual term, the core of negative residuals coinciding with the core of convective area of a cloud cluster. Hence, the predominantly negative values in Fig. 3c can be explained as due to the cumulus activities in the depression region. The patterns of these vorticity budget terms



for Depression 3 are similar to those for Depression 1.

Next, we examine in detail the contributions of various terms in the vorticity equation to the movement of monsoon depressions. For this, all terms (eq. (1)), were computed over an area  $6.5^\circ$  longitude  $\times$   $11^\circ$  latitude on the eastern half, as well as on the western half of the three depressions, and the averages for the two halves were obtained. The grid points along a north-south direction passing through the center of the depression were not included. Figs. 4a-e are vertical sections of the vorticity divergence term, horizontal advection term, vertical advection term, tilting term and residual terms respectively on the eastern and western halves of Depression 1. On comparison of vorticity divergence term and horizontal advection term (Figs. 4a, b), one finds that the two terms have an opposite effect on vorticity generation in lower levels. The vorticity divergence term is negative in the western half and positive in the eastern half at 850 and 700 mb. This means an increase in vorticity in the western half and a decrease in the eastern half resulting in the westward movement of the depression. In contrast, the horizontal advection term is positive in the western half and negative in the eastern half (at lower levels) which is indicative of a depression moving eastward. This result was expected for the following reason. The rainfall, and hence upward motion/convergence, is largest in the southwest sector of a typical monsoon depression. As the vorticity is almost symmetric on both halves, the vorticity divergence, which is negative on both sides, has a greater magnitude in the western half. In the case of horizontal advection, as the easterlies are weaker than westerlies in a monsoon depression, the vorticity advected to the eastern half is greater at least in the lower levels (1000 and 850 mb). Daggupati and Sikka obtained similar results. Also, Rao and Rajamani (1970) using a quasi-geostrophic model inferred that at the 850 mb level, the divergence term caused westward movement whereas the horizontal advection term caused eastward movement. Considering higher levels (600 mb and above), on the western half of the depression both terms are predominantly negative and on the eastern side predominantly positive. Therefore, the depression would move westwards. The vertical

advection and tilting terms have similar patterns on both sides (Figs. 4c, d), resulting in no influence on the movement in the east-west direction. In Fig. 4e we see that the residual term acts as a vorticity sink at lower levels (negative values of the residual term result from decrease in vorticity) on both halves, but is positive at levels at and above 700 mb (up to 12 August) in the eastern half and negative in the western half. Therefore, due to this term, which is due to cumulus scale effects and fractional effects, the depression would move eastwards. Another aspect the residual term noted is the predominant negative values in the western half compared to the eastern half. We know that for a typical monsoon depression, there is more intense cumulus activity in the southwestern sector or in the western half than in the eastern half. This further corroborates the inference of Sui and Yanai (1986) that negative residuals in the vorticity budget equation are associated with cumulus convective region.

Depression 1 (6-13 August) moved west-northwestwards whereas Depression 2 (10-15 August) moved northwards. Therefore, by comparing the terms of the vorticity equation from both halves of both depressions one brings out the differences if any in the contributions of each term to the westward movement of the depression. Figs. 5a-e are for Depression 2. Fig. 5a, the vorticity divergence term, is mostly negative (increases in vorticity) in the western half and mostly positive (or decrease in vorticity) in the eastern half, resulting in westward movement of the depression. However the contrast in the two halves is not as much as in Fig. 4a. In Fig. 5b the horizontal advection term is mostly positive in the western side and mostly negative in the eastern side, which would cause eastward movement of the depression. This is in contrast to the case of Depression 1, where advection term (Fig. 4b) caused the westward movement of the depression above the 600 mb level.

In Figs. 5c and 5d the vertical advection term and tilting term have the same pattern on both halves and as a result do not contribute to the movement in the east-west direction. As in the case of Depression 1 (Figs. 4c, 5c), the vorticity sink is in the lower levels and vorticity source in the upper levels due to vertical advection term, while there is a reversed pattern due to the tilting

term (Fig. 5d) in case of Depression 2. The terms in the case of Depression 3 (5–9 July 1979) are similar to those of Depression 1. To sum up, by comparing the two depressions (Figs. 4a–e and 5a–e) we see that the vorticity divergence term at most of the levels and the horizontal advection term at levels above 600 mb cause westward movement of the depression.

### 3.2. Energetics of the monsoon circulation

To see how the monsoon systems are maintained, we computed the energy of the various

monsoon systems and the energy conversions between them. The computations were made over a limited region from  $69^{\circ}\text{E}$  to  $150^{\circ}\text{E}$ , and from  $7.5^{\circ}\text{N}$  to  $30^{\circ}\text{N}$  which cover the possible tracks of the monsoon depressions and the monsoon trough.

*3.2.1. Equations for energetics.* Studies on the energetics of limited regions during the summer monsoon were made by for example Krishnamurti et al. (1976), Murakami (1977) and Rajamani (1985). The equations for energy terms and energy-transformation terms are (following

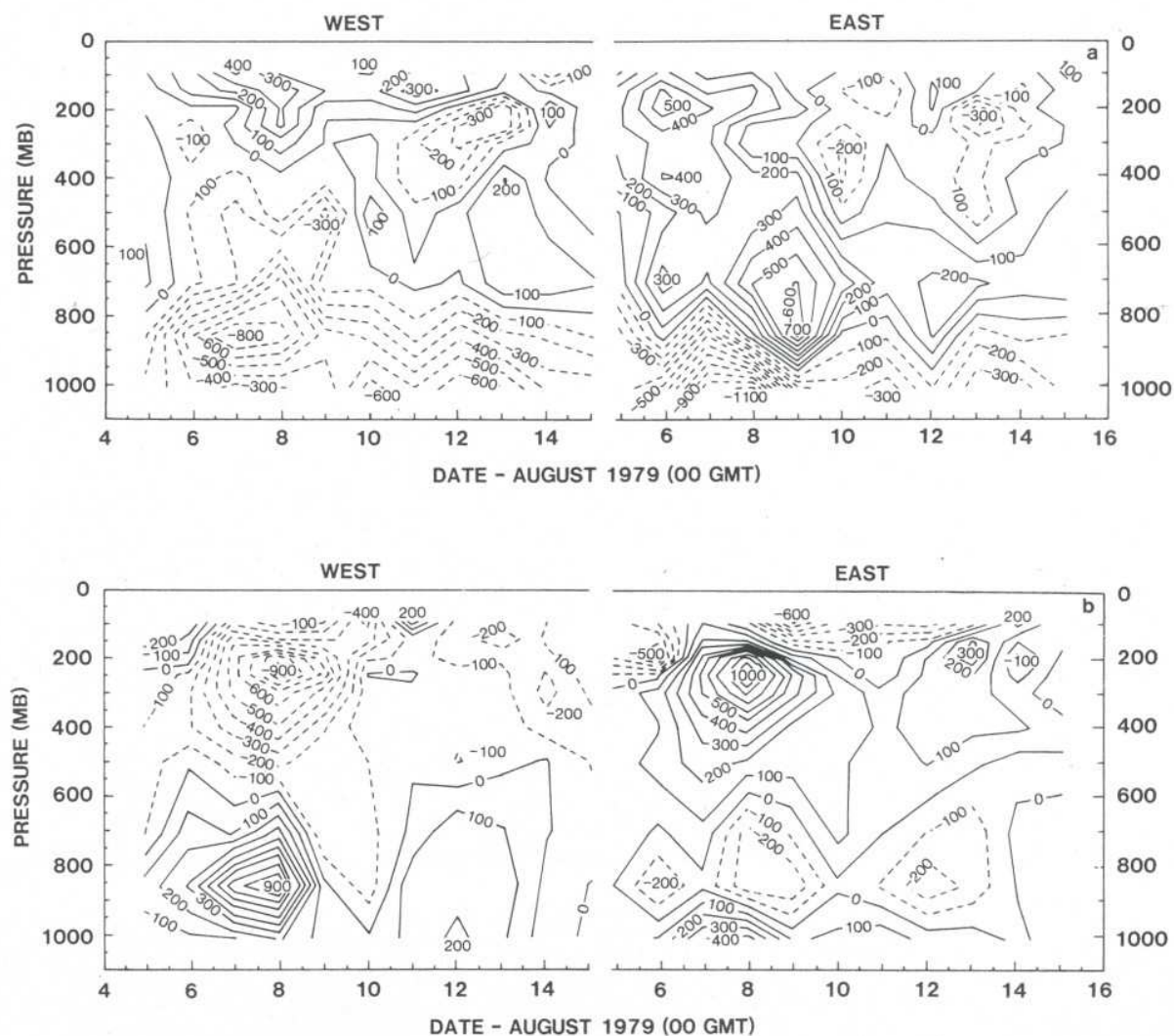


Fig. 4. Height-time section for Depression 1. The eastern and western sectors: (a) the vorticity divergence term; (b) horizontal advection term; (c) the vertical advection term; (d) the tilting term; (e) the residual term. The units are  $10^{-12} \text{ s}^{-2}$ .



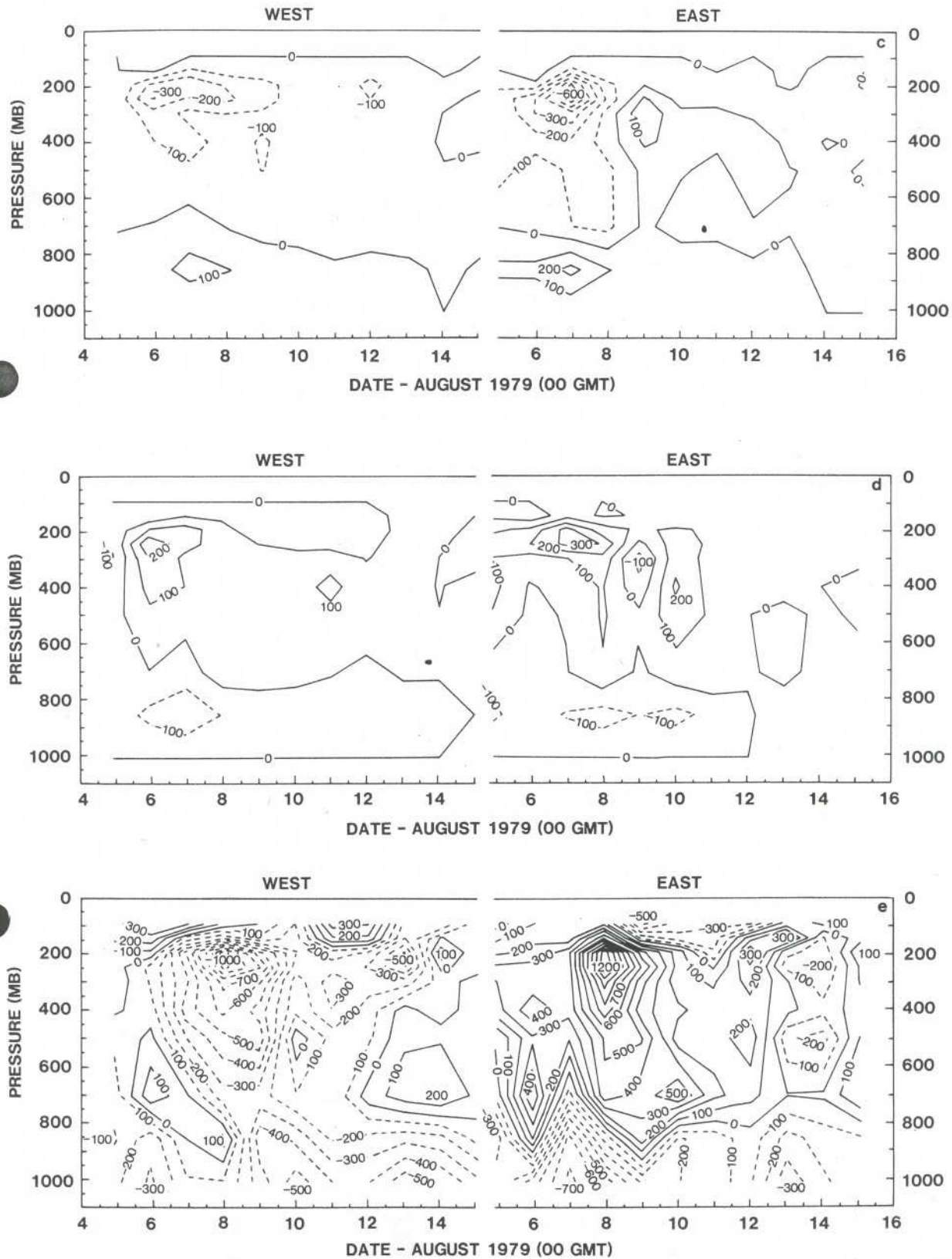


Fig. 4 (cont'd).

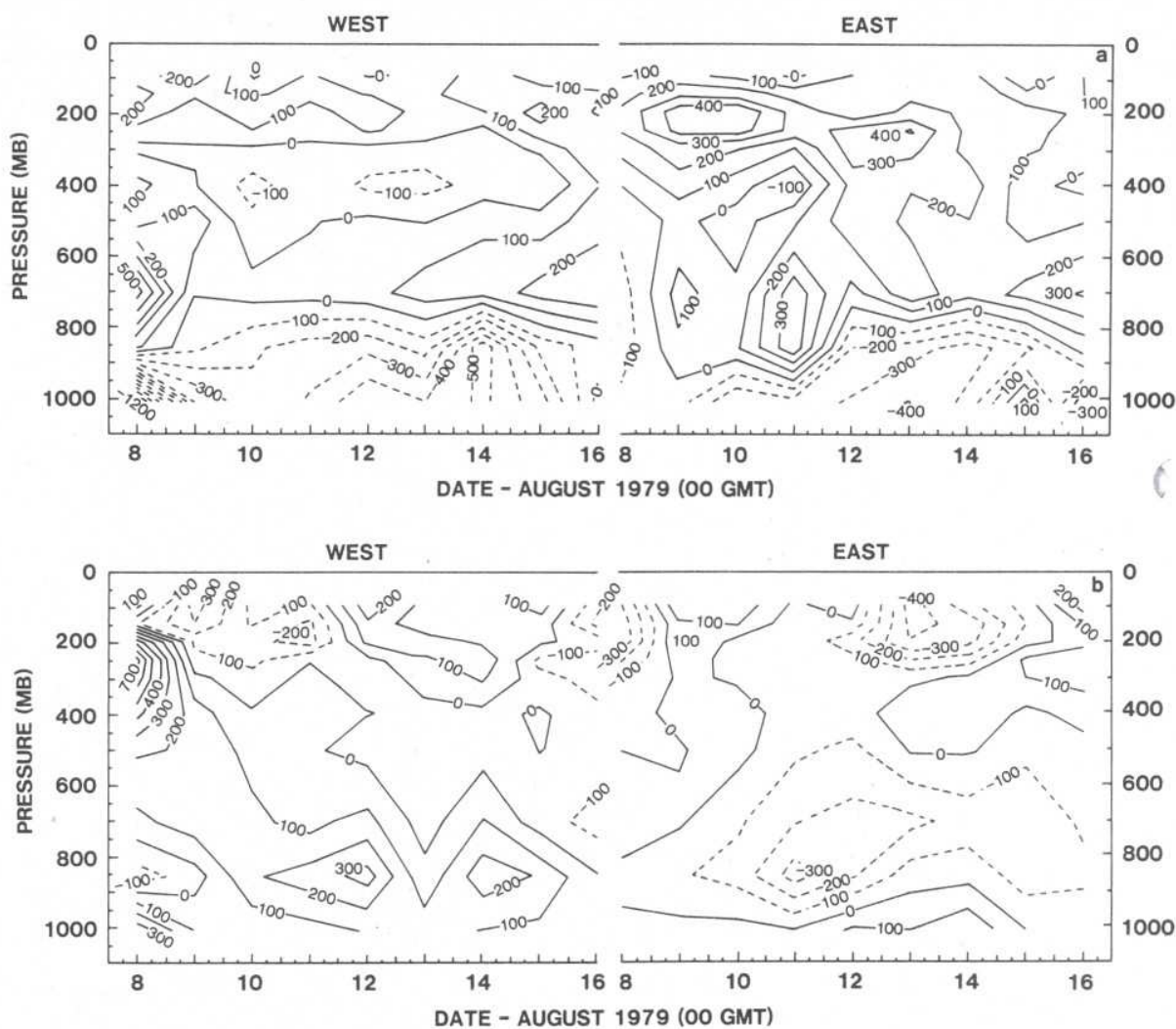


Fig. 5. Height-time section for Depression 2 (10–15 August 1979) for the eastern and western sectors: (a) a vorticity divergence term; (b) the horizontal advection term; (c) the vertical advection term; (d) the tilting term; (e) the residual term. The units are  $10^{-12} \text{ s}^{-2}$ .

Lorenz, 1955; Oort, 1964; Smith, 1969; Tripoli and Krishnamurti, 1975; and Murakami, 1977):

$$A_z = \frac{C_p}{2} \int_M \gamma ([T] - \bar{T})^2 dM, \quad (1a)$$

$$A_E = \frac{C_p}{2} \int_M \gamma [T^{*2}] dM, \quad (2)$$

$$K_z = \frac{1}{2} \int_M ([u]^2 + [v]^2) dM, \quad (3)$$

$$K_E = \frac{1}{2} \int_M ([u^{*2}] + [v^{*2}]) dM, \quad (4)$$

$$C(A_z, A_E) = -C_p \int_M \gamma \left\{ [v^* T^*] \frac{\partial}{\partial y} [T] + [\omega^* T^*] \frac{\partial}{\partial p} [T] \right\} dM, \quad (5)$$

$$C(A_z, K_z) = -R \int_M \frac{1}{p} ([\omega] - \{\omega\}) \times ([T] - \{T\}) dM, \quad (6)$$

$$C(A_E, K_E) = -R \int_M \frac{1}{p} [\omega^* T^*] dM, \quad (7)$$

$$C(K_z, K_E) = - \int_M \left\{ [u^* v^*] \frac{\partial}{\partial y} [u] + [u^* \omega^*] \frac{\partial}{\partial p} [u] + [v^* \omega^*] \frac{\partial}{\partial p} [v] + [v^* v^*] \frac{\partial}{\partial y} [v] \right\} dM, \quad (8)$$



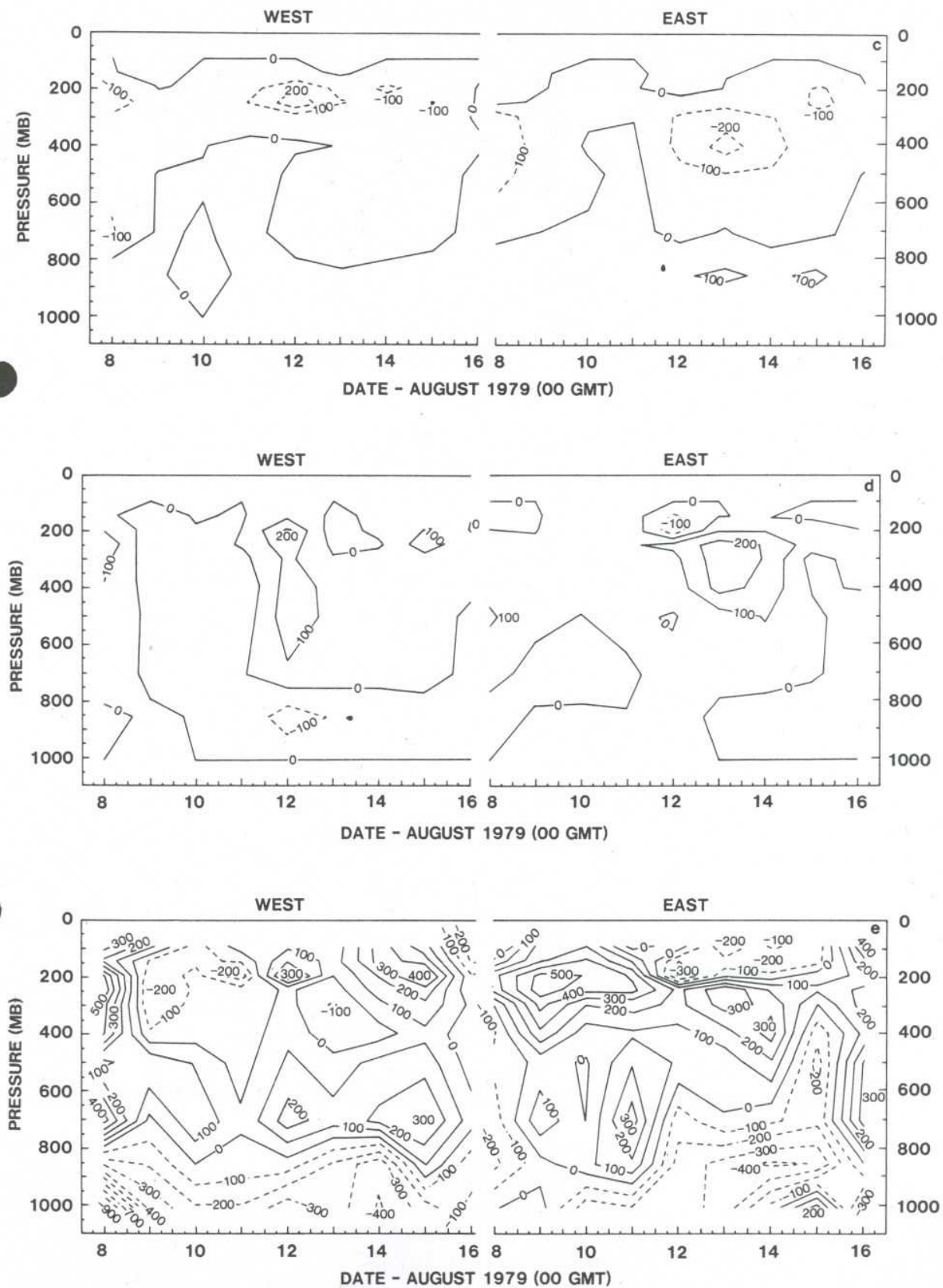


Fig. 5 (cont'd).

where

$$\gamma = -\frac{\theta}{T} \frac{R}{C_p P} \left( \frac{\partial \bar{\theta}}{\partial p} \right)^{-1}$$

and  $M$  is the mass of the atmosphere over the area under study, square brackets, the zonal mean and a star deviation from the zonal mean (other symbols have the usual meaning). In this study, instead of computing  $A_z$ , the zonal available potential energy (which involves global seasonal mean temperature  $\bar{T}$ ), we computed  $A_{zc}$ , the baroclinic contribution of available potential energy (Smith, 1969), the variation of which is more relevant to the present study. This would be referred to as zonal available potential energy for brevity.  $A_{zc}$  is given by:

$$A_{zc} = \frac{C_p}{2} \int_M \gamma ([T] - \{T\})^2 dM. \quad (1b)$$

$T$  is the temperature averaged over the limited region of interest.

As we are dealing with a limited region, eqs. (5)–(8) do not exactly represent the energy transformations. We intended to determine the direction of energy conversions in order to understand how various monsoon systems are maintained in a broad sense rather than to make energy budget studies. Therefore, we believe that the use of eqs. (5)–(8) is justifiable. Here the eddies are both the monsoon depressions (or lows) and the monsoon trough.

**3.2.2. Discussion on energetics.** The vertical time section of the energy terms is seen in Figs. 6a–d. The important point is the high values of energy at 300–200 mb levels and the minimum values in the mid troposphere (500–400 mb). Both zonal and eddy kinetic energy (Figs. 6c, d) have higher values on 7 and 8 August when Depression 1 was most intense. Also there are slightly higher values on 11–13 August corresponding to Depression 2.

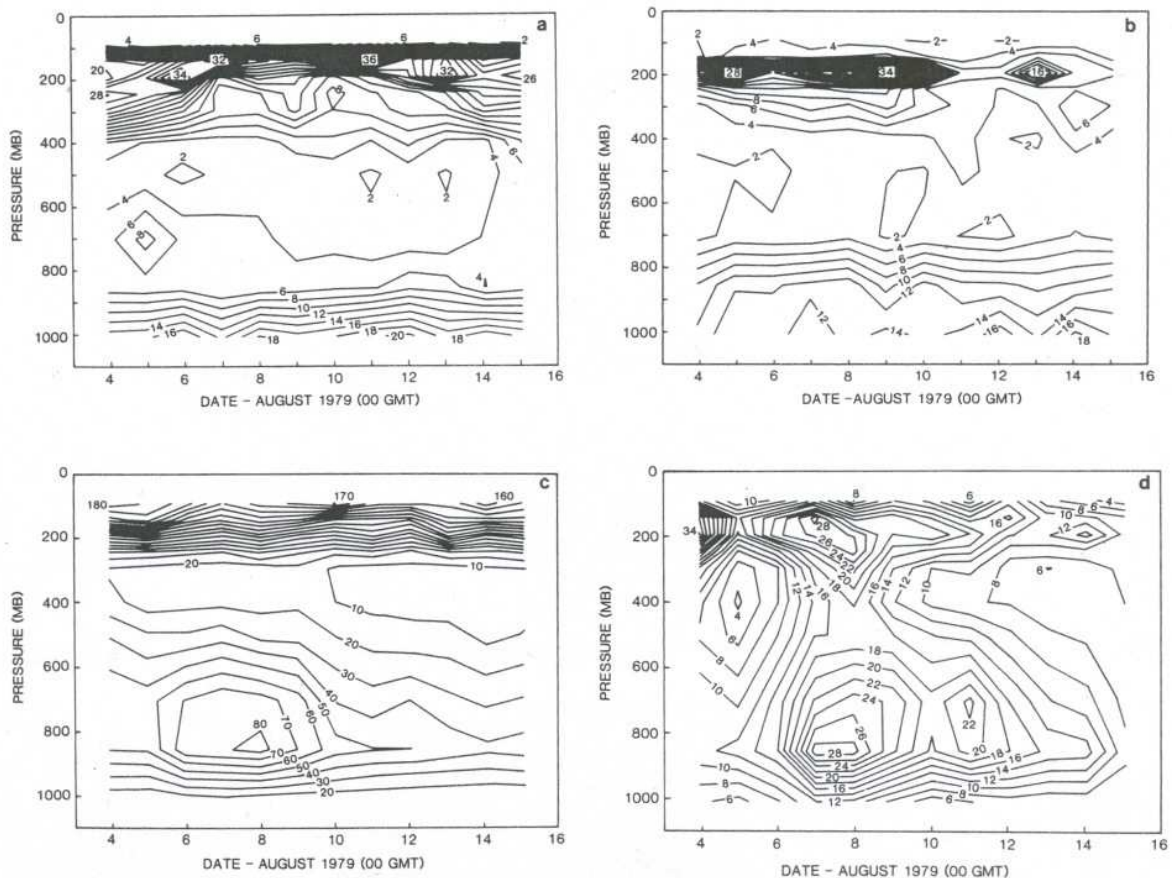


Fig. 6. Height-time section of (a) the zonal available potential energy; (b) eddy available potential energy; (c) zonal kinetic energy; (d) eddy kinetic energy. The units are  $m^2 s^{-2}$ .



The variation in time of the vertically integrated energy conversion terms for the period from 4–15 August 1979 is seen in Figs. 7a–d. The conversion of available potential energy is mostly from zonal current (which is proportional to the north–south temperature variance) to the eddies due to sensible heat transport down the gradient. Also, frequently eddy available potential energy is converted into eddy kinetic energy (Fig. 7b) by the rising of warm air and sinking of cold air. Moorthi and Arakawa (1985) have also investigated theoretically baroclinic instability with cumulus heating for basic zonal flows similar to the summer monsoon flow. They found the conversions to be from zonal available potential energy to eddy available potential energy and from eddy available potential energy to eddy kinetic energy. We see similar conversion rates to increase until 7 August, when Depression 1 was most intense (Fig. 7). Thereafter, the rates decreased with a secondary maximum on 12 August when Depression 2 was active. The zonal current gained kinetic energy from the eddies (Fig. 7c) until 8 August when Depression 1 reached its peak in intensity. Thus, when the depression was strengthening, it also provided energy to the zonal current. This is in agreement with observations that whenever monsoon lows/depressions form and intensify, the monsoon current also strengthens. Also, from Fig. 7 we see that zonal kinetic energy is converted into zonal available potential energy because of rising of cold air or sinking of warm air due to orographic effect and/or due to dynamical effect of the synoptic

conditions. Similarly, the conversion rates of available potential energy from zonal current to eddies are about an order of magnitude greater than those of other conversion terms.

Figs. 8a–d is a plot of the time variation of the energy terms and that of the total gain (or loss) of the energy terms due to the conversions. In general, the variations in the energy terms follow the gain or loss due to the conversions, and therefore, the conversion terms have a dominant rôle. In addition, the zonal available potential energy decreases with the strengthening of the depression, eddy available potential energy, zonal kinetic energy and eddy kinetic energy increase with strengthening of the depression and decrease with weakening (Figs. 8a–d).

In summary, the following features are observed during the life cycle of the monsoon depression. The monsoon systems contain maximum energy at the 300–200 mb levels with a secondary maximum at the 850–700 mb levels. The eddy available potential energy, the zonal kinetic energy, the eddy kinetic energy and the energy conversion rates all increase with the strengthening of the monsoon depression, and then start decreasing during weakening of the system. The zonal available potential energy, which is proportional to the north–south temperature variance, is the main source of energy. This is converted on most days into eddy available potential energy which, in turn, is converted into eddy kinetic energy on most days. The eddies and the zonal current strengthen simultaneously and the direction of energy conversion between them alternates. Lastly, the zonal kinetic energy is more often converted into zonal available potential energy.

**3.2.3. Transport of momentum.** By examining the vertical-latitude section of the transport of momentum for the period from 4–15 August, we suggest that “negative momentum transport” or the southward transport of westerly momentum over the region from 18°N to 25°N increases with the strengthening of the depression reaching maximum amount of transport on 7 August, when it was most intense. At that time there is a convergence of westerly momentum around 20°N. Thereafter, the northward transport of momentum dominates. For example on 9 August, over the region 12°N to 20°N, there is northward transport and consequently the westerlies south

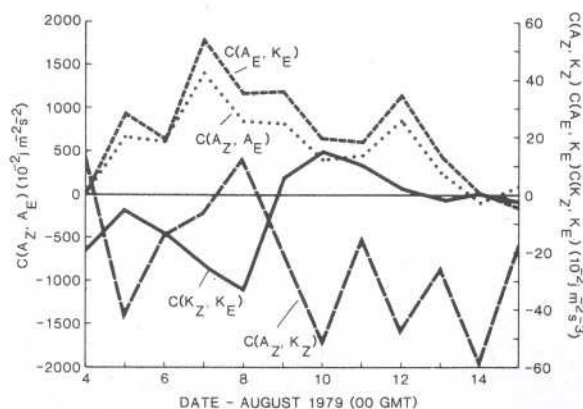


Fig. 7. Vertically integrated conversion rates ( $10^{-2} \text{ J m}^{-2} \text{ s}^{-1}$ ).

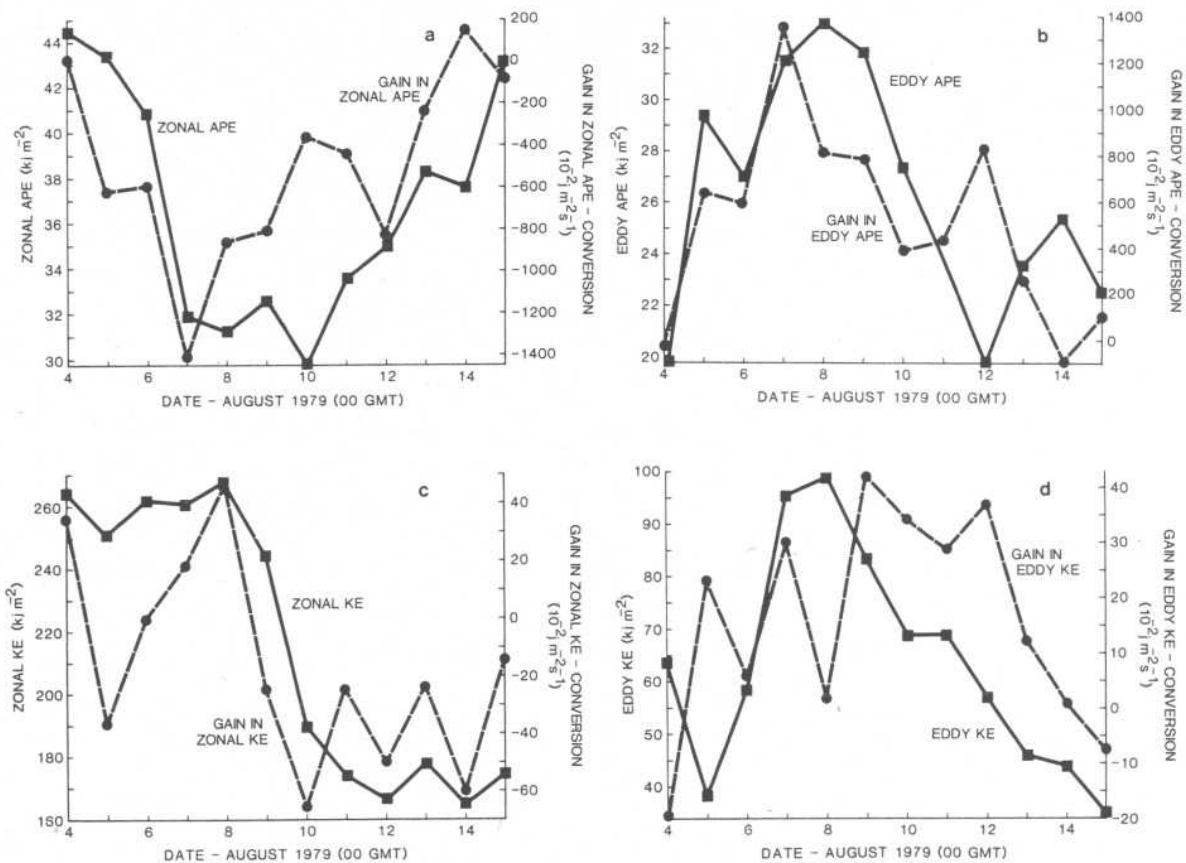


Fig. 8. Vertically integrated energy terms ( $\text{kJ m}^{-2}$ ) and gain/loss due to conversions ( $10^{-2} \text{ J m}^{-2} \text{ s}^{-1}$ ). (a) Zonal available potential energy; (b) eddy available potential energy; (c) zonal kinetic energy; (d) eddy kinetic energy.

of the monsoon trough, that is, of  $20^\circ\text{N}$  or so weakens. Figs. 9a-d is a plot of the vertical-latitudinal section of transport of momentum for different stages of the depression, viz., growing stage (4 August), most intense stage (7 August) and decaying stage (9, 11 August). From this, we see that during the growth of the system southward transport occurs over the region  $18^\circ\text{N}$  to  $25^\circ\text{N}$  and during the decay period northward transport occurs.

**3.2.4. Thermal structure.** The temperature anomaly in the field of depression was computed in the following way. The zonally averaged temperatures at all latitudes were subtracted from the temperature field over the depression area in order to remove the trend of north-south temperature gradient. Temperature anomalies averaged at the four grid points surrounding the center of depression were considered as the tem-

perature anomaly at the center. This was carried out at all levels for the period from 4-12 August. Fig. 10 is a plot of the vertical time section of these temperatures. From 5-8 August, when the depression intensified, it has a warm core with a maximum warming of  $2^\circ\text{C}$  at 700 mb. There is another maximum having a value of  $3^\circ\text{C}$  at 200 mb level. After 9 August, the warm core is replaced by a cold core with a maximum cooling of  $1^\circ\text{C}$ . This cooling may be due to evaporation.

In earlier studies, Krishnamurti et al. (1975) observed that the August 1968 depression had a cold core in the lower troposphere and warm core in the upper troposphere. In 1977 Godbole (1977b) obtained similar results. However, Nitta and Masuda (1981) have found that the 5-9 July 1979 depression had a warm core based on their computations extending up to 500 mb level; this is consistent with our results.



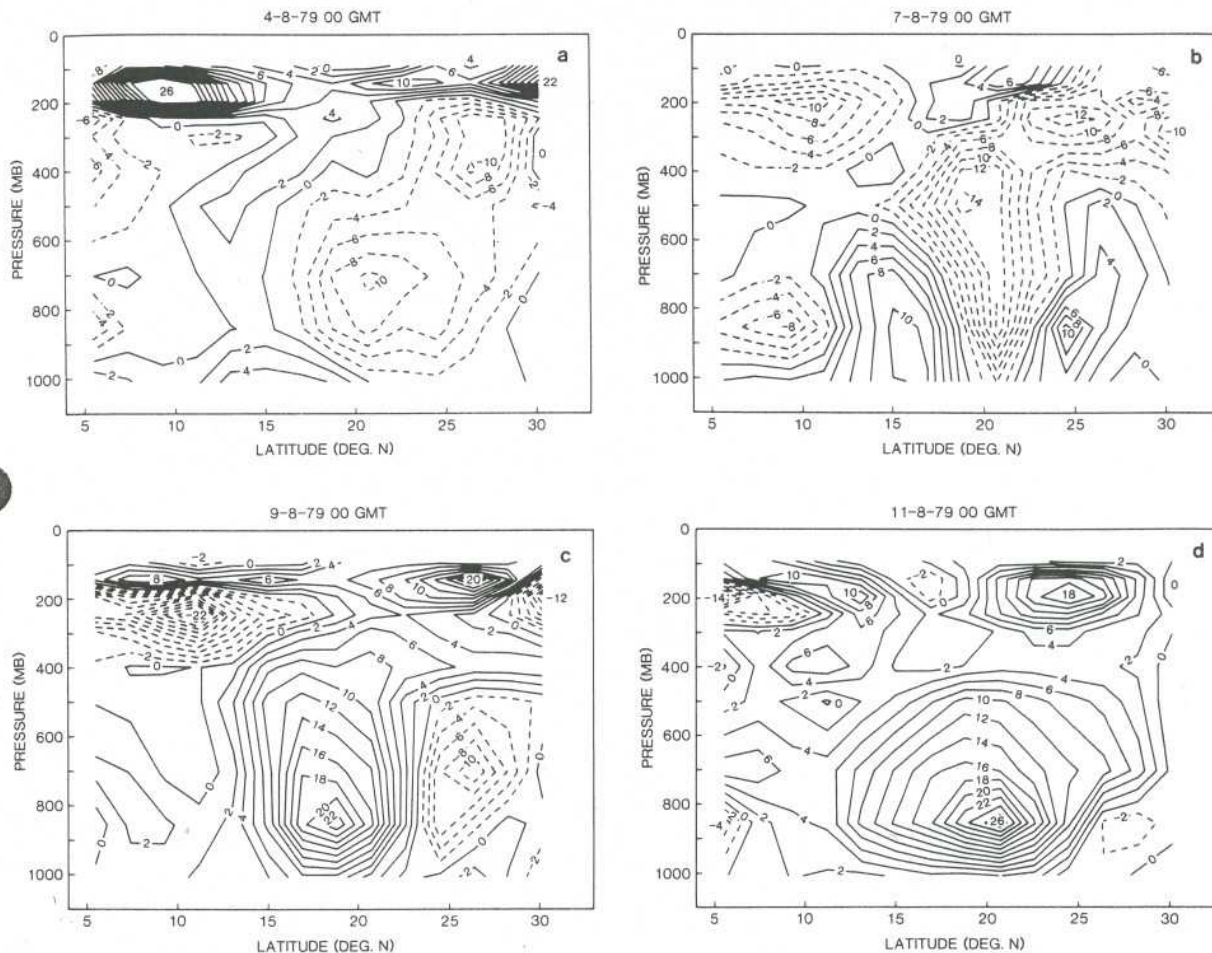


Fig. 9. Momentum transport ( $\text{m}^2 \text{s}^{-2}$ ). (a) 4 August 1979; (b) 7 August 1979; (c) 9 August 1979; (d) 11 August 1979.

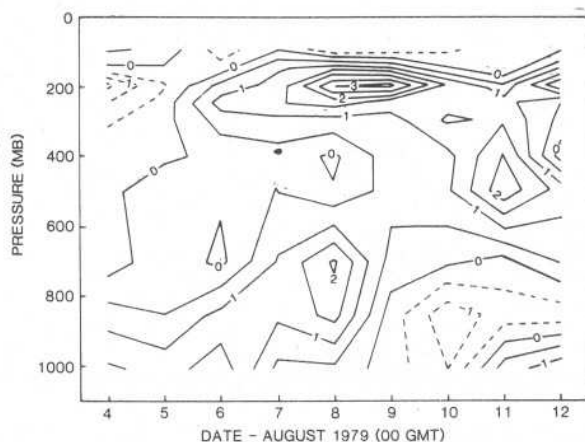


Fig. 10. Temperature anomaly ( $^{\circ}\text{C}$ ) for depression (4-12 August 1979).

#### 4. Concluding remarks

Over its life cycle Depression 1 (6-13 August) was most intense at the 700 mb level. The mean

relative vorticity over the depression field had a maximum value of  $3.3 \times 10^{-5} \text{ s}^{-1}$  on 7 August. When the depression merged with seasonal low, the maximum value was at the 1000 mb level. The maximum vertical velocity was  $1.7 \text{ cm s}^{-1}$  on 7 August. At low levels the vorticity divergence term contributed to the westward movement of the depression whereas horizontal advection term contributed to the eastward movement. However, both terms together contributed to the westward movement at higher levels. Predominant negative values of the residual term are observed for Depression 1 in the western half compared to the eastern half. As for a typical monsoon depression, cumulus convective activity is stronger in the western half, this corroborates the inference that the large residuals in the vorticity budget are associated with intense cumulus convection (Sui and Yanai, 1986). At 1000 mb, the residual is negative (vorticity sink) in both halves of the

three depressions. This may be attributed to the surface friction. Neither the vertical advection term, nor the tilting term contributed significantly to the movement in the east-west direction. The former acted as a vorticity sink at low levels and vorticity source at upper levels; the opposite is true with the latter. Although both terms are small they cannot be neglected, particularly during the disturbed period.

The energy terms have higher values at 300–200 mb levels and also at 850–700 mb values. The eddy available potential energy, zonal and eddy kinetic energy increase with the strengthening of the depression. The zonal available potential energy or the north–south temperature variance supplies available potential energy to the eddies; the eddy available potential energy on most of the days is converted into eddy kinetic energy which maintains the zonal current.

We also inferred that during the strengthening

of the monsoon depression, the transport of momentum is southward in the region from 18°N to 25°N and during decay of the system, the transport is northward. The depression had a warm core with a positive temperature anomaly of 2°C at 700 mb level and about 3°C at 200 mb level during the intense period of the depression. Two days after the peak intensity, it became cold core with a negative temperature anomaly of 1°C.

## 5. Acknowledgements

The research reported in this paper was supported by the National Science Foundation under Grant No. ATM 8419735. Partial support for the senior author and computer usage came from the Graduate School of the University of Wisconsin-Milwaukee.

## REFERENCES

- Chen, G. T. J. and Bosart, L. F. 1979. A quasi-Lagrangian vorticity budget of composite cyclone-anticyclone couplets accompanying north American polar air outbreaks. *J. Atmos. Sci.* 36, 185–194.
- Chen, G. T. J. and Chang, C. P. 1980. The structure and vorticity budget of an early summer monsoon trough (Mei-Yu) over southeastern China and Japan. *Mon. Wea. Rev.* 110, 137–152.
- Daggupaty, S. M. and Sikka, D. R. 1977. On the vorticity budget and vertical velocity distribution associated with the life cycle of a monsoon depression. *J. Atmos. Sci.* 5, 773–792.
- DiMego, G. J. and Bosart, L. F. 1982. The transformation of tropical storm Agnes into an extra tropical cyclone. Part II. Moisture, vorticity and kinetic energy budgets. *Mon. Wea. Rev.* 110, 412–433.
- Douglas, M. W. 1987. The structure and dynamics of monsoon depressions. *FSU Report No. 86-15*, Dept. of Meteorology, FSU, Tallahassee, 1–273.
- Godbole, R. V. 1977a. On cumulus-scale transport of horizontal momentum in monsoon depression over India. *Monsoon Dynamics* (ed. T. N. Krishnamurti). *PAGEOPH* 115, 1373–1382.
- Godbole, R. V. 1977b. The composite structure of the monsoon depression. *Tellus* 29, 25–40.
- Krishnamurti, T. N. 1985. Summer monsoon experiment—a review. *Mon. Wea. Rev.* 113, 1590–1626.
- Krishnamurti, T. N., Kanamitsu, M., Godbole, R. V., Chang, C. B., Carr, F. and Chow, J. H. 1975. Study of a monsoon depression. I. Synoptic structure. *J. Meteor. Soc. Japan* 53, 227–239.
- Krishnamurti, T. N., Kanamitsu, M., Godbole, R. V., Chang, C. B., Carr, F. and Chow, J. H. 1976. Study of a monsoon depression. II. Dynamical structure. *J. Meteor. Soc. Japan* 54, 208–225.
- Lorenz, E. N. 1955. Available potential energy and the maintenance of the general circulation. *Tellus* 7, 157–167.
- Moorthi, S. and Arakawa, A. 1985. Baroclinic instability with cumulus heating. *J. Atmos. Sci.* 42, 2007–2030.
- Murakami, T. 1977. Regional energetics over the north Pacific, south China Sea and the Indonesian seas during winter. *Monsoon Dynamics* (ed. T. N. Krishnamurti). *PAGEOPH* 115, 1283–1301.
- Nitta, T. and Masuda, K. 1981. Observational study of a monsoon depression developed over the Bay of Bengal during summer MONEX. *J. Meteor. Soc. Japan* 59, 672–682.
- Nitta, T. and Murakami, T. 1980. Three dimensional structure and energy cycles of a monsoon depression developed over the Bay of Bengal, Part A, *WMO* 9, FGGE Operational Report, 137–144.
- Oort, A. H. 1964. On estimates of the atmospheric energy cycle. *Mon. Wea. Rev.* 92, 483–493.
- Rajamani, S. 1985. Energetics of the monsoon circulation over south Asia. II. Energy terms and energy transformation terms. *Mausam* 36, 405–412.
- Rao, K. V. and Rajamani, S. 1970. Diagnostic study of a monsoon depression by geostrophic baroclinic model. *Ind. J. Meteor. Geophys.* 21, 187–194.
- Rao, Y. P. 1976. Southwest monsoon, meteorological



- monograph. *Synoptic Meteorology No. 1/1976*. India Meteorological Dept., 1-367.
- Reed, R. J. and Johnson, R. H. 1974. The vorticity budget of synoptic scale wave disturbances in the tropical western Pacific. *J. Atmos. Sci.* 31, 1784-1791.
- Saha, K. R. and Shukla, J. 1980. Further evidence of association of westward propagating disturbances with monsoon disturbances, Part A, *WMO 9, FGGE Operations Report*, 23-31.
- Sanders, F. 1984. Quasi geostrophic diagnosis of the monsoon depression of 5-8 July 1979. *J. Atmos. Sci.* 41, 538-552.
- Sikka, D. R., Rajamani, S. and Singh, S. S. 1980. Life cycle of a monsoon depression in the Bay of Bengal 3-9 July 1979, results of summer MONEX field phase research, Part A, *WMO 9, FGGE Operations Report*, 129-133.
- Sikka, D. R. and Grossman, R. 1980. *Summer MONEX chronological weather summary*. International MONEX Management Center, India Meteorological Department, New Delhi-3, India.
- Smith, P. J. 1969. On the contribution of a limited region to the global energy budget. *Tellus* 21, 202-207.
- Sui, C. H. and Yanai, M. 1986. Cumulus ensemble effects on the large-scale vorticity and momentum fields of GATE. Part I. Observational evidence. *J. Atmos. Sci.* 43, 1618-1642.
- Surgi, N. 1984. The structure and dynamics of a monsoon depression. *Proceedings of 15th Conf. on Hurricanes and Tropical Meteorology*, held at Miami, FL, 9-13 January 1984, A.M.S., 354-358.
- Tripoli, G. J. and Krishnamurti, T. N. 1975. Low-level flows over the GATE area during summer 1972. *Mon. Wea. Rev.* 103, 197-216.
- Warner, C. 1984. Core structure of a Bay of Bengal monsoon depression. *Mon. Wea. Rev.* 112, 137-152.
- W.M.O. 1981. Summer MONEX Field Phase Report. *FGGE Operations Report*, vol. 8.